



Chinese Society of Aeronautics and Astronautics  
& Beihang University

Chinese Journal of Aeronautics

cja@buaa.edu.cn  
www.sciencedirect.com



# Aerodynamic force and moment measurement of 10° half-angle cone in JF12 shock tunnel



Yunfeng LIU\*, Yunpeng WANG, Chaokai YUAN, Changtong LUO, Zonglin JIANG

State Key Laboratory of High Temperature Gas Dynamics, Institute of Mechanics, Chinese Academy of Sciences, Beijing 100190, China

Received 26 April 2016; revised 13 May 2016; accepted 27 May 2016  
Available online 14 February 2017

## KEYWORDS

Aerodynamic force and moment measurement;  
10° half-angle cone model;  
JF12;  
Real-gas effects;  
Shock tunnel

**Abstract** An aerodynamic force and moment measurement was conducted in JF12 long-test-duration detonation-driven shock tunnel of Institute of Mechanics, Chinese Academy of Sciences. The test duration of JF12 is 100–130 ms. The nominal Mach number is 7.0 and the exit diameter of the contoured nozzle is 2.5 m. The total enthalpy is 2.5 MJ/kg which duplicates the hypersonic flight conditions of Mach number 7.0 at 35 km altitude. The test model is the standard aerodynamic force model of 10° half-angle sharp cone. The length of the test model is 1500 mm and the weight is 57 kg. The aerodynamic forces were measured with a six-component strain balance. The angles of attack were set to be  $-5^\circ$ ,  $0^\circ$ ,  $5^\circ$ ,  $10^\circ$  and  $14^\circ$ , respectively. The experimental results show that in the 100–130 ms test duration, the signals of strain balance have 3–4 complete vibration cycles. So, the aerodynamic forces and moments can be obtained directly by averaging the signals of balance without acceleration compensation. The force measurement error of repeatability of JF12 is less than 2%. The aerodynamic force coefficients of JF12 are in good agreement with those of conventional hypersonic wind tunnels. For this test model at Mach number 7.0 and total enthalpy of 2.5 MJ/kg, the real-gas effects on aerodynamic force characteristics are not very evident.

© 2017 Chinese Society of Aeronautics and Astronautics. Production and hosting by Elsevier Ltd. This is an open access article under the CC BY-NC-ND license (<http://creativecommons.org/licenses/by-nc-nd/4.0/>).

## 1. Introduction

Conventional hypersonic wind tunnels usually produce test flows with low total temperature and low sound speed; there-

fore, the thermochemical reaction, one of the key mechanisms in hypersonic flows, is ignored in its experiments. As a result, the real-gas effects on the aerodynamic force and moment measurement become a very difficult problem in the hypersonic ground tests and were identified as an unknown “unknown”.<sup>1</sup> During the first entry flight of the Space Shuttle Orbiter at Mach number  $Ma = 24$  and 70 km altitude, the vehicle exhibited an extra nose-up pitching moment increment relative to the preflight prediction. Woods et al.<sup>2</sup> noted that preflight prediction based on the perfect aerodynamics in the Aerodynamic Design Data Book indicated that a  $7.5^\circ$  deflection of the body flap would be required to trim the Space

\* Corresponding author.

E-mail address: [liuyunfeng@imech.ac.cn](mailto:liuyunfeng@imech.ac.cn) (Y. LIU).

Peer review under responsibility of Editorial Committee of CJA.



Shuttle Orbiter. However, in reality, the body flap had to deflect to a large value of about  $\delta \approx 16^\circ$  to maintain trim at the attack angle of  $\alpha = 40^\circ$ . The deflection angle of  $16^\circ$  was close to the possible deflection limitation and more deflection would lead to a big flight test accident. Comparison of equilibrium-air computations with perfect gas model indicated that at least the main mechanism of the so-called hypersonic anomaly was due to real-gas effects at very high Mach numbers.<sup>3</sup>

At an enthalpy of about 3 MJ/kg or higher, air molecules become vibrationally excited, dissociated, and ionized behind a shock wave. These real-gas phenomena absorb heat. As a result, the effective specific heat ratio decreases and compressibility increases. These phenomena cause changes in pressure distribution, and thereby aerodynamic characteristics of the hypersonic vehicle. To design an efficient hypersonic vehicle, the influence of real gas effects on force and moment must be known accurately. To experimentally verify the accuracy of those design parameters, wind tunnel tests are needed. To produce flows with desired temperature, Mach number and Reynolds number in the test section, such tunnels must be operated at very high enthalpies and reservoir pressures.<sup>4,5</sup>

In order to improve the accuracy of the ground experimental data, various advanced hypersonic test facilities were developed.<sup>6-8</sup> One of the main concerns was related to the aerodynamic force and moment during hypersonic vehicle reentry. Unfortunately, there is no single ground-based facility capable of duplicating the hypersonic flight environment, and so far different facilities are used to address various aspects of the design problems associated with hypersonic flight.<sup>9</sup> Considering the thermochemistry in hypersonic flows, high-enthalpy shock tunnels are capable of generating high-temperature flows, but its effective test duration is too short to do force and moment measurement. Moreover, for hypersonic experiments, there is not any reliable scaling criterion available between the low speed wind tunnel tests and the real flights.<sup>10,11</sup>

Under the support of National Major Project of Scientific Instrumentation Research and Development, a super-large detonation-driven shock tunnel was developed based on backward-running detonation driver in Institute of Mechanics, Chinese Academy of Sciences in 2012.<sup>12</sup> It was named as JF12 long-test-duration shock tunnel, where “J” means shock wave and “F” means wind tunnel in Chinese, and 12 is its series number. It has the capability of reproducing pure airflows with Mach numbers from 5 to 9 at altitude of 25–50 km. More importantly, it has a test duration of more than 100 ms which makes it the first shock tunnel in the world to conduct aerodynamic force and moment measurement by using traditional strain gage balances. The second large shock tunnel in the world is the LENSII shock tunnel, which has a test time of about 30 ms.<sup>13</sup>

The force and moment measurement of hypersonic vehicles is one of the main long-term research projects of JF12 shock tunnel in order to study the aerodynamic characteristics under real-gas conditions. In this paper, as the first step of this project, we conducted the force and moment measurement of  $10^\circ$  half-angle sharp cone standard model at Mach number 7.0 under the duplicated hypersonic flight conditions of about 35 km altitude with the total enthalpy of 2.5 MJ/kg. The aim of this paper is to examine whether JF12 can be used to conduct force measurement and obtain high-accuracy data. The

primary experimental results are given and compared with conventional hypersonic wind tunnel results. This research will be continued further in JF12 shock tunnel under high enthalpy conditions.

## 2. Experimental setup and test model

The diagram of JF12 long-test-duration shock tunnel is shown in Fig. 1. The total length of the facility is 265 m. It consists of 5 main parts. From right to left, they are E-shape vacuum tank and test section, nozzle, driven section, detonation driver section and damping section. The vacuum tank has a volume of about  $600 \text{ m}^3$  with a length of 40 m. The diameter of the test section is  $\varnothing 3.5 \text{ m}$ . The contoured nozzle is 15 m long with an exit diameter of  $\varnothing 2.5 \text{ m}$ . The nominal Mach numbers are 5–7 with exchangeable throats. The driven section is 89 m in length and  $\varnothing 720 \text{ mm}$  in inner diameter. The detonation driver is 99 m in length and  $\varnothing 400 \text{ mm}$  in inner diameter. The driver is operated in the backward-running detonation mode, that is, the detonation is ignited at its right end and propagated to the left. The detonation driver and the driven section are connected with a transition section by which the tube diameter is gradually reduced from  $\varnothing 720 \text{ mm}$  to  $\varnothing 400 \text{ mm}$ . There is a diaphragm rig between the detonation driver and the transition section, which is used to produce the proper incident shock wave in the shock tunnel after the direct detonation initiation. The damping section is located at the left end of the facility, which is 19 m in length and  $\varnothing 400 \text{ mm}$  in inner diameter. The role of this part is to avoid the damage of the detonation front to the facility. Fig. 2 is the photo of JF12 shock tunnel.

The test model is a  $10^\circ$  half-angle sharp cone and it is a standard aerodynamic force model. There are many experimental results obtained in conventional hypersonic wind tunnels to be compared with. The length of the model is 1.5 m with a base diameter of  $\varnothing 528 \text{ mm}$ . It is made of aluminum alloy and weighs 57 kg. Fig. 3 is the photo of test model installed in JF12 shock tunnel. Pressure transducers were also installed on the bottom surface to measure the base pressure of the model during the experiments. The bottom of the test model is shown in Fig. 4.

A six-component stress balance specially designed for JF12 shock tunnel was used to measure the aerodynamic force and moment. Fig. 5 shows the photo of this balance. The maximum diameter of this balance is  $\varnothing 100 \text{ mm}$ . In the JF12 shock tunnel experiments, the mechanical vibration of the test model, the balance and the sting will not be damped within the test time of 100 ms. Therefore, the balance output signals contain inertial force. In order to reconstruct the force and moment from the balance output signals and obtain high-quality data, we must make sure that we can get at least 3–4 complete vibration periods in the 100 ms test time. Therefore, the balance was designed with high stiffness. In addition, the strength of the sting and model supporting system was also strengthened.

Before the wind tunnel experiments, the vibration frequency of model supporting system of JF12 shock tunnel was measured by dynamic calibration with fracture-stick technique. The model supporting system includes the model, the balance, the sting and the supporting equipment. The sting was made of alloy steel with a diameter of  $\varnothing 100 \text{ mm}$ . The vibration frequency in the normal direction was recorded by

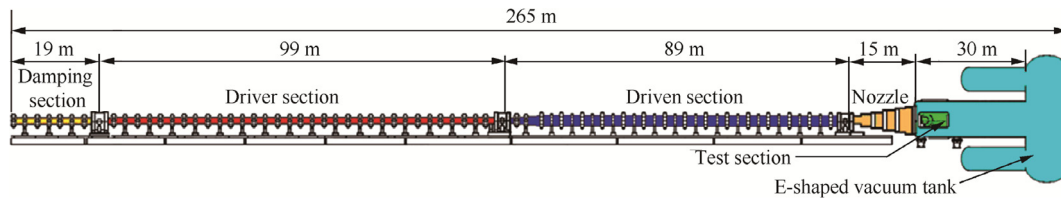


**Fig. 1** Schematic of JF12 long-test-duration detonation-driven shock tunnel.



**Fig. 2** Photo of JF12 long-test-duration shock tunnel.



**Fig. 5** Six-component stress balance designed for JF12 shock tunnel.



**Fig. 3** 10° half-angle cone model installed in JF12 shock tunnel.

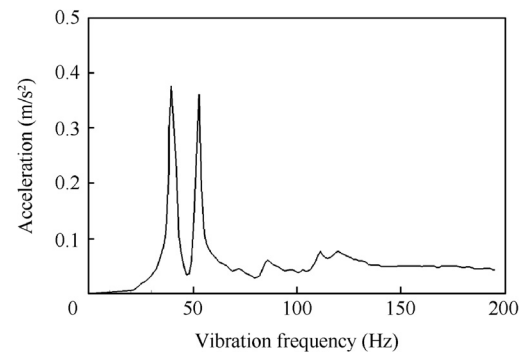


**Fig. 6** Vibration frequency of JF12 model supporting system.

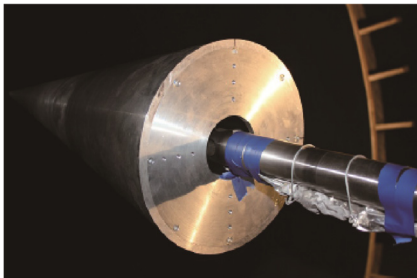


**Fig. 4** Pressure transducers installed on bottom surface of test model.

accelerometers and the results are shown in Fig. 6. From Fig. 6, we can see that the first order modal frequency is 40 Hz, which means that we can get at least four complete vibration periods in the normal force direction within 100 ms test time. In the axial force direction, the first order modal frequency is more than 100 Hz. So, at least ten complete vibration periods can be obtained in 100 ms test time.

In this study, the nominal Mach number is  $Ma = 7.0$ . The total enthalpy is 2.5 MJ/kg and the total pressure is 3.0 MPa,

which duplicates the flight conditions at about 35 km altitude. The test conditions were monitored by Pitot probes in each run. The free stream is assumed to be in equilibrium and the parameters were calculated by considering real-gas effects in the stagnation chamber. The angles of attack  $\alpha$  were set to be  $-5^\circ$ ,  $0^\circ$ ,  $5^\circ$ ,  $10^\circ$  and  $14^\circ$ , respectively. The angle of sideslip was zero. The runs at  $5^\circ$  angle of attack were repeated six times and the runs at other angles of attack were repeated three times in order to study the repeatability precision of force and moment measurement in JF12 shock tunnel.

### 3. Results and discussion

The typical output signals of the balance are shown in Fig. 7, including the axial force, normal force and pitching moment. It can be seen clearly that the balance signals can be divided into two parts. At the first 30 ms, the signals are irregular, which means that the model undertakes irregular mechanical vibration. This is caused by the unsteady establishment process of the flow field. The time duration of this flow field establishment process depends on many parameters, such as the shape

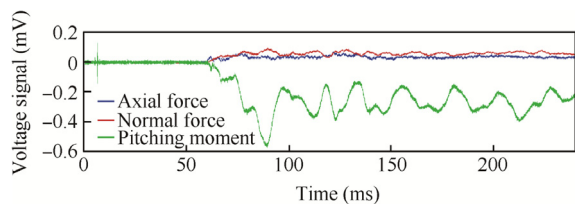


Fig. 7 Balance output signals of JF12 shock tunnel.

and size of the model, the angle of attack and the Mach number. This unsteady starting process can also be confirmed by the base pressure signals of the model, which are shown in Fig. 8 here. Therefore, the results in this starting process cannot be used to calculate the aerodynamic force and moment.

After the unsteady starting process, the output signals of the balance become regular and there are at least three complete periodical cycles within the 100 ms test duration. The forces measured by the balance contain aerodynamic force and inertia force. The inertia force can be easily removed by averaging the balance signals. Therefore, we do not need to use acceleration compensation method to reconstruct the aerodynamic forces and moments.<sup>14,15</sup> It means that the highly accurate data could be obtained with this stress balance by applying simple data processing techniques. As to the axial force, its high-frequency oscillations make sure that there are more than 10 periodical cycles to achieve highly accurate data. The periodicity of the balance signal data from the JF12 shock tunnel indicates that its accuracy could be as high as that of conventional hypersonic wind tunnels. However, the data accuracy will be ruined if the wind tunnel test time is shorter than 30 ms for this test model or the frequency of the natural vibration mode of the force measurement system of JF12 shock tunnel is lower than 10 Hz.

The normal force coefficients  $C_n$  and axial force coefficients  $C_a$  at different attack angles are plotted in Figs. 9 and 10. The average results of FD-07, FD-03 and Langley 11-in. conventional low-enthalpy hypersonic wind tunnels are also shown in these figures for comparison.<sup>16</sup> All the JF12 experimental results are plotted in these figures, while only the average results of other wind tunnels are given. The coefficients of pressure center  $X_{cp}$  are plotted in Fig. 11. First of all, we can find that the force measurement data of JF12 shock tunnel has high repeatability precision. The repeatability error of normal force coefficient is less than  $\pm 0.6\%$ . The repeatability error of axial force coefficient is less than  $\pm 1.5\%$ . There are two key techniques to guarantee that high-quality experimental data can be obtained. The first key technique is the detonation-driven technique. Detonation-driven shock tunnel can produce high-quality flow field because it is independent of the rupture pressure of the metal diaphragm, while in other shock tunnels, the rupture process of diaphragm influences the flow field very

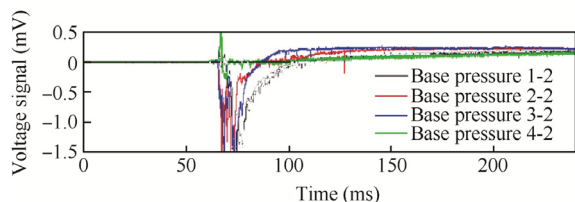


Fig. 8 Base pressure signals of JF12 shock tunnel.

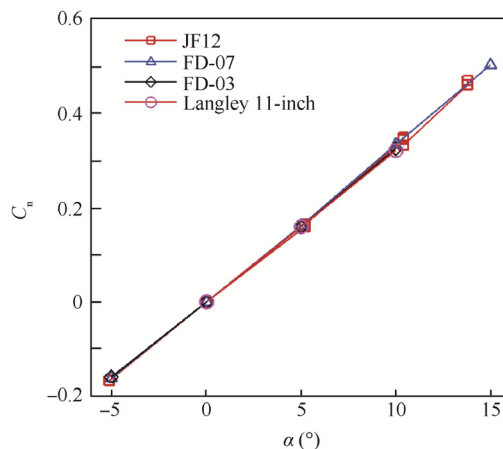


Fig. 9 Normal force coefficients at different angles of attack.

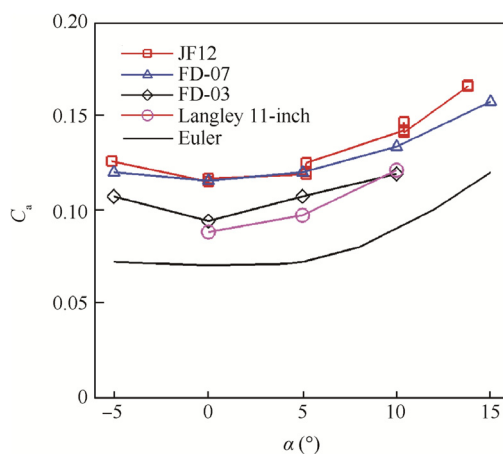


Fig. 10 Axial force coefficients at different angles of attack.

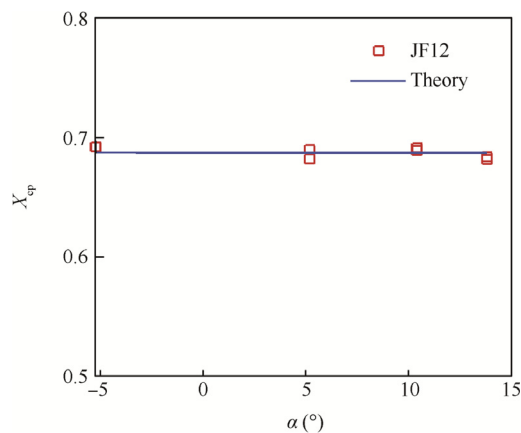


Fig. 11 Coefficients of pressure center at different angles of attack.

much. The second key technique is the long test duration. In the 100 ms long test duration, the data in the unsteady starting process can be easily discarded. The model has 3–5 complete vibration periods and the inertia force can be easily removed by averaging the balance signals.

From Figs. 9 and 11, we can see that normal force coefficients  $C_n$  of JF12 at different angles of attack agree very well with the results of other conventional hypersonic wind tunnels with a discrepancy of less than 1%. The coefficient of pressure center  $X_{cp}$  is also in accordance with the theoretical result of  $X_{cp} = 0.6874$ . The axial force can be divided into two parts: one is the pressure force and the other is the friction force. In Fig. 10, the axial force coefficients calculated by Euler equations are also shown. The difference between the experimental results and Euler results is the friction force coefficients. For the laminar boundary layer, the friction force coefficient is inversely proportional to the square root of the Reynolds number  $Re_L$  based on the length of the model.

The axial force coefficients of FD-03 and Langley are almost the same. The axial force coefficient of JF12 is about 10% higher than that of FD-03 because the  $Re_L$  of FD-03 is about two times that of JF12. The  $Re_L$  of JF12 is about  $1.5 \times 10^6$  and the  $Re_L$  of FD-03 is about  $3 \times 10^6$ . The friction force is about 10% of the total axial force for FD-03 and about 20% of the total axial force for JF12. For FD-07, its  $Re_L$  is about  $5 \times 10^6$  and boundary layer transition occurs at the aft part of the model.<sup>16</sup> Therefore, its axial force coefficients become larger than those of FD-03 and similar to those of JF12 at lower angles of attack.

#### 4. Conclusions

Aerodynamic force and moment measurements of a  $10^\circ$  half-angle sharp cone model were carried out in JF12 shock tunnel at Mach number 7.0 under the duplicated hypersonic flight conditions of about 35 km altitude. The results show that high-accuracy force measurement data can be obtained in JF12 shock tunnel. The maximum repeatability error is less than 2%. The experimental results are in good agreement with those of conventional hypersonic wind tunnels. The discrepancy of normal force coefficients between JF12 and conventional hypersonic wind tunnels is less than 1%. The discrepancy of axial force coefficients between JF12 and conventional tunnels is caused by the different Reynolds numbers based on the length of model. For the simple configuration of  $10^\circ$  half-angle sharp cone under total enthalpy of 2.5 MJ/kg, the real-gas effects on the aerodynamic characteristics are not very evident.

#### Acknowledgements

The authors would like to thank all the members of JF12 research group for their invaluable support. This research

was supported by the National Natural Science Foundation of China (Nos. 11672312, 11532014).

#### References

- Bertin JJ, Cummings RM. Critical hypersonic aerothermodynamic phenomena. *Ann Rev Fluid Mech* 2006;**38**(1):129–57.
- Woods WC, Arrington JP, Hamilton HH. A review of preflight estimates of real-gas effects on space shuttle aerodynamic characteristics. *Shuttle performance: Lessons learned*. Washington, D.C.: NASA Conference Publication; 1983.
- Maus JR, Griffith BJ, Szema KY, Best JT. Hypersonic mach number and real gas effects on space shuttle orbiter aerodynamic. *J Spacecraft Rockets* 1984;**21**(2):136–41.
- Park C. Hypersonic aerothermodynamics: Past, present and future. *Int'l J of Aeronautical & Space Sci* 2013; **14**(1):1–10.
- Park C. Evaluation of real-gas phenomena in high-enthalpy impulse test facilities: A review. *Journal of Thermophysics and Heat Transfer* 1997;**11**(1):10–8
- Lu FK, Marren DE. Advanced hypersonic test facilities. *Prog Astronaut Aeronaut* 1971;**1**:64.
- Abbott CD, Mickle EJ, Brooks WK. Status of AEDC transonic, supersonic, and hypersonic wind tunnel improvement programs. Reston: AIAA. 2012. Report No.: AIAA-2012-3172.
- Tang ZG, Xu XB, Yang YG, Li XG, Dai JW, Lyu ZG, et al. Research progress on hypersonic wind tunnel aerodynamic testing techniques. *Acta Aeronaut Astronaut Sin* 2015;**36**(1):86–97 [Chinese].
- Bertin JJ, Cummings RM. Fifty years of hypersonics: where we've been, where we're going. *Prog Aerospace Sci* 2003;**39**(6–7):511–36.
- Bushnell DM. Scaling: Wind tunnel to flight. *Annu Rev Fluid Mech* 2006;**38**:111–28.
- Chen JQ, Zhang YR, Zhang YF, Chen LZ. Review of correlation analysis of aerodynamic data between flight and ground prediction for hypersonic vehicle. *Acta Aerodynamica Sin* 2014;**32**(5):587–99 [Chinese].
- Jiang Z, Yu H. Experiments and development of long-test-duration hypervelocity detonation-driven shock tunnel (LHDst). Reston: AIAA. 2014. Report No.: AIAA-2014-1012.
- Dufrene A, MacLean M, Wadhams T, Holden M. Extension of LENS shock tunnel test times and lower mach number capability. Reston: AIAA. 2015. Report No.: AIAA-2015-2017.
- Luo YF, Bi ZX. The accelerometer force balance used in the impulse wind tunnel. *Aerodynamic Exp Meas Control* 1996;**10**(1):59–63 [Chinese].
- Sahoo N, Mahapatra DR, Jagadeesh G. An accelerometer balance system for measurement of aerodynamic force coefficient over blunt bodies in a hypersonic shock tunnel. *Measurement Science and Technology* 2003;**14**:260–72.
- Chen H. Investigation on the link-up between the aerodynamic force data measured in supersonic and hypersonic wind tunnel. *Acta Aerodynamica Sin* 2002;**18**(3):345–9 [Chinese].